Metal Ion Adsorption and Electrocrystallization

By W. J. Lorenz, E. Schmidt, G. Staikov † and H. Bort

Institut für Physikalische Chemie und
Elektrochemie der Universität Karlsruhe, Germany
and
Institut für Anorganische, Analytische und
Physikalische Chemie der Universität Bern, Switzerland

Received 4th August, 1977

Deposition of lead onto silver single crystal electrodes from perchlorate solutions has been studied in the undervoltage and low overvoltage regions employing twin-electrode thin layer and potential pulse techniques. Pseudo-Nernstian θ isotherms exhibiting continuous coverage steps were found. 2D nucleation was not identified to be a kinetically relevant process. The rate of 3D nucleation decreases with increasing θ, thus indicating major structural dissimilarities between the 2D layer and the 3D nuclei.

INTRODUCTION

It is well known that in the initial stages of numerous metal electrocrystallization processes taking place at foreign solid substrates, considerable amounts of the electroactive cation, Me^{z+}, are deposited at potentials more positive than the Me^{z+}/Me_{bulk} equilibrium potential, building up strongly adsorbed (sub)monolayers at the electrode/electrolyte interphase.[1,2] Interest in these effects has grown remarkably during the last years as it became clear from the work of several authors[3–6] that the kinetic and equilibrium properties of the emerging deposits are markedly influenced by the crystallographic orientation of the substrate electrode.

There is now widespread (although not unanimous) belief that undervoltage deposition should be interpreted in terms of a nucleative epitaxial mechanism[3–5] assuming the Me^{z+} layer to originate in a sequence of 2D phase transitions initiated by discrete two dimensional nucleation acts. Subsequent lateral growth eventually would result in the formation of ordered adsorption structures in registry with the substrate lattice whose stability is restricted to well defined potential intervals within a more or less extended undervoltage range. Besides determining the shape of the pertinent adsorption isotherms, ordered coverages thus produced might also play decisive roles within the growth mechanism of Me bulk phase deposits, providing for a suitable 3D nucleation environment or even acting as a precursor matrix of developing lattice planes.

It has been pointed out,[7] however, that 2D nucleation (which, of course, conflicts rather sharply with any continuous Me^{z+} adsorption model brought forward previously[1,8]), is still far from being unambiguously confirmed by experiment as a metal undervoltage mechanism of universal relevance.

In order to acquire a more coherent picture of the low-coverage behaviour of a selected system, Pb deposition onto Ag single crystals from perchlorate solutions has

† Permanent address: Institute of Electrochemical Power Sources, Bulgarian Academy of Science, Sofia, Bulgaria.

been studied in the undervoltage and low-overvoltage regions. This choice of the system was motivated by both the absence of complex formation in the Pb^{2+}/ClO_4^- couple [9] and the inability of the perchlorate ion to adsorb specifically at Ag substrates.[10] Consequently, the observed polarization phenomena are supposed to be indicative of the interactions between the substrate and the Me coverage proper, undisturbed by chemical complications and competitive or co-adsorption effects.

The experiments performed include charge and coverage determinations by the concentrostatic twin-electrode thin layer method [11] as well as potential pulse experiments at chemically polished single crystal surfaces. For additional voltammetric and morphological studies Ag substrates made electrolytically by the Budevski capillary method [12] were used.

In this paper, a brief account of the results obtained is given. Experimental details will be reported elsewhere.[13–15]

UNDERVOLTAGE PROPERTIES OF THE Pb^{2+}, ClO_4^-/Ag SYSTEM

COVERAGE ISOTHERMS

Voltammetric twin-electrode thin layer experiments have been carried out with chromate-polished [16] Ag single crystals of (100), (110) and (111) orientation, using bulk Pb as a Pb^{2+} reversible generator electrode.[11]

Typical undervoltage voltammograms are shown in fig. 1. At the low potential sweep rates employed ($|dE/dt| < 1$ mV s^{-1}), there is reasonable symmetry between the

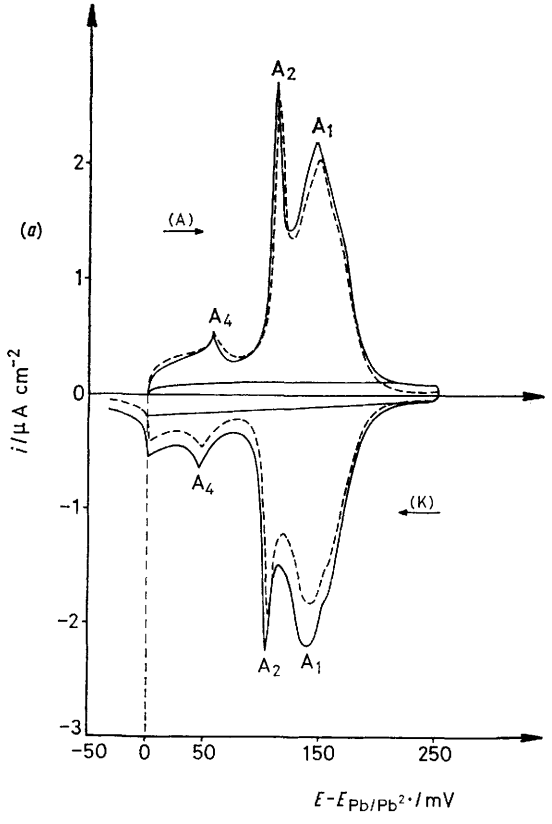

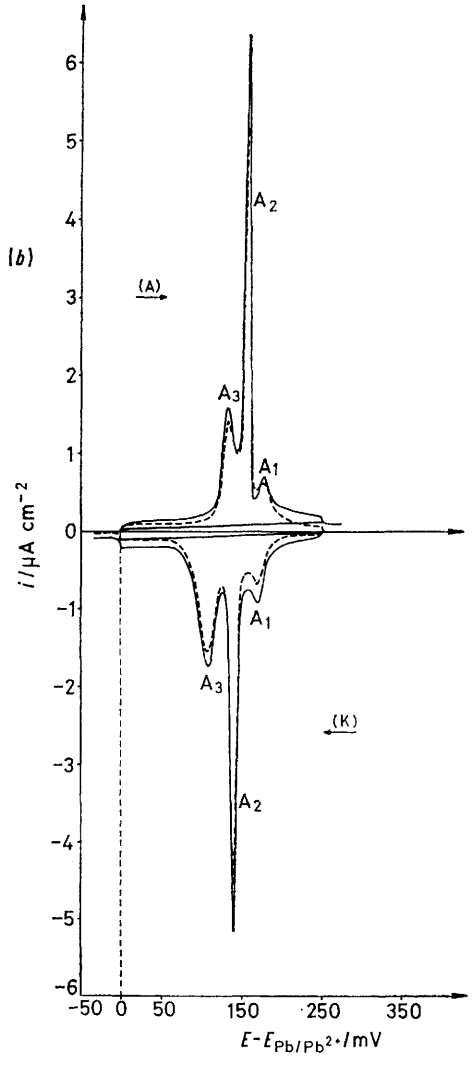

FIG. 1.—Twin-electrode thin layer voltammograms of the Pb^{2+}, ClO_4^-/Ag(*hkl*) system. (*a*) Ag(100); (*b*) Ag(111). Electrolyte: 0.5 mol dm^{-3} $NaClO_4$ + 0.005 mol dm^{-3} $HClO_4$ + 2×10^{-4} mol dm^{-3} Pb^{2+}; chromate-polished electrode surfaces; $T = 298$ K; $|dE/dt| = 0.42$ mV s^{-1}. (A), anodic curves; (K), cathodic curves. —— i; - - - - - i_g.

anodic and cathodic current curves, indicating reversibility of the undervoltage process at the time scale of the experiment. In all systems, multiple peak structures have been found (table 1), the main peaks being A_1 and A_2 at the (100) and (110), and A_2 at the (111) crystal faces, respectively. The peak potentials obtained agree fairly well with the corresponding values reported by Bewick[17] and by Dickertmann *et al.*[18]

According to the operating principle of the twin electrode method, the current, i, measured at the Me adsorbing electrode, corresponds to the global charge flux due to the variation of the surface charge density, whereas the generator current, i_g, is equivalent to the amount of Pb^{2+} deposited per unit time. Assuming equilibrium to have been established at the initial and final potentials, E_a and E_e, of a given voltage scan,

surface charge and Pb surface concentration increments may be determined simply by integrating the corresponding i and i_g voltammograms:

$$\Delta q = q_{(E_e,\ c_{Pb^{2+}})} - q_{(E_a,\ c_{Pb^{2+}})} = -\int_{E_a}^{E_e} i\ dt \tag{1}$$

$$\Delta\Gamma_{Pb} = \Gamma_{Pb(E_e,\ c_{Pb^{2+}})} - \Gamma_{Pb(E_a,\ c_{Pb^{2+}})} = (2F)^{-1}\int_{E_a}^{E_e} i_g\ dt. \tag{2}$$

TABLE 1.—UNDERVOLTAGE PEAK POTENTIALS OF THE Pb^{2+}, ClO_4^- + Ag(hkl) SYSTEM

	A_1/mV	A_2/mV	A_3/mV	A_4/mV
Ag(110)	169	140	—	25
Ag(100)	146	111	—	46
Ag(111)	169	152	128	—

From $\Delta q/\Delta\Gamma_{Pb}$ correlations thus obtained the charge/coverage coefficient of the Pb undervoltage deposit,

$$Z_E = F^{-1}(\partial q/\partial\Gamma_{Pb})_E, \tag{3}$$

is calculated. Z_E is found to coincide with the Pb^{2+} ionic charge within the limits of experimental accuracy:[15]

$$Z_E = 2 \pm 0.1\ [Pb^{2+},\ ClO_4^-/Ag\ (100);\ (110);\ (111)]. \tag{4}$$

This implies that in analogy with the Pb^{2+}/ClO_4^- system with polycrystalline electrodes,[11] Pb^{2+} is the only ionic species substantially incorporated into the inner double layer.

Procedure (2) results in a direct $\Delta\Gamma$ determination which in contrast to charge-coverage evaluations of conventional single electrode voltammograms, does not depend on *a priori* suppositions with respect to Z_E. Because Γ_{Pb} is likely to vanish if $E \longrightarrow \infty$ in the absence of specific anion adsorption, absolute Γ_{Pb} data are obtained by eqn (2) provided that a sufficiently high starting potential, E_a, is applied:

$$\Gamma_{Pb(E,c_{Pb^{2+}})} = \lim_{E_a\to\infty} (2F)^{-1}\int_{E_a}^{E} i_g\ dt. \tag{5}$$

The experimental limit values of Γ_{Pb} thus determined with E approaching the Pb_{bulk}/Pb^{2+} equilibrium potential, $E_{Pb/Pb^{2+}}$, consistently come close to the packing density of the bulk Pb (111) lattice plane, allowing for a roughness factor of ~1.2:

$$\lim_{E\to E_{Pb/Pb^{2+}}} \Gamma_{Pb(E,c_{Pb^{2+}})} \equiv \Gamma_{s,Pb} \approx 1.7 \sim 1.9\ \text{nmol cm}^{-2}\ \text{(table 2)}. \tag{6}$$

TABLE 2.—EXPERIMENTAL AND HYPOTHETICAL Pb SURFACE CONCENTRATIONS (CHARGE EQUIVALENTS)

	$2F\Gamma$/mC cm^{-2}
$\Gamma_{s,Pb}$ Ag(110) exp.	0.38 ± 0.02
$\Gamma_{s,Pb}$ Ag(100) exp.	0.37 ± 0.02
$\Gamma_{s,Pb}$ Ag(111) exp.	0.34 ± 0.02
Pb(111) calc.	0.302
Ag(111) — 3(2 × 2)Pb calc.	0.336
Ag(100) — c(2 × 2)Pb calc.	0.193
Ag(100) — c(2 × 2)Pb — c(2 × 2)Pb calc.	0.386

Hence one might speculate that in the Pb layer at potentials near $E_{Pb/Pb^{2+}}$, a similar close packed structure is present.[17] Notice, however, that as a consequence of the rather large Ag/Pb misfit, which is of the order of 20%, close-packed arrangements of Pb atoms cannot be planar in direct contact with any Ag crystal face unless some non-spherical deformation of either the substrate, or part of the adsorbate particles is permitted. In the Ag(100) system, $\Gamma_{s,Pb}$ would also be compatible with a square twin-layer $c(2 \times 2) - c(2 \times 2)$ structure.[13]

Due to the nearly ideal q/Γ stoichoimetry as expressed by eqn (4), unified $c_{Pb^{2+}}$-independent coverage isotherms are produced with each crystal orientation when the

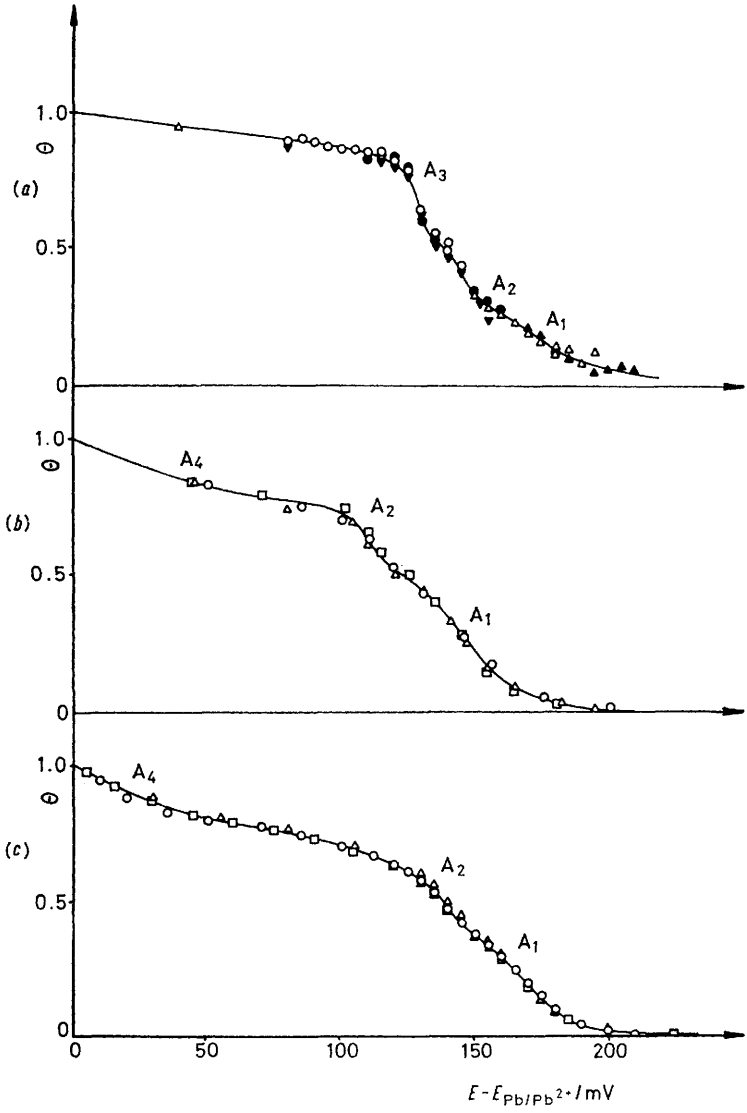

FIG. 2.—Coverage isotherms $\theta_{(E-E_{Pb/Pb^{2+}})}$ of the Pb^{2+}/ClO_4^- system. Electrolyte: 0.5 mol dm^{-3} $NaClO_4$ + 0.005 mol dm^{-3} $HClO_4$ + x mol dm^{-3} Pb^{2+} ($10^{-4} < x < 10^{-3}$). (*a*) Ag (111)/Pb^{2+}, (*b*) Ag(100) Pb^{2+}, (*c*) Ag(110) Pb^{2+}.

experimental set of Γ_{Pb} data (normalized with respect to $\Gamma_{s,Pb}$) as obtained for different $c_{Pb^{2+}}$ values, is plotted against the undervoltage, $E - E_{Pb/Pb^{2+}}$:

$$\Gamma_{Pb(E,c_{Pb^{2+}})}/\Gamma_{s,Pb} = \theta_{(E - E_{Pb/Pb^{2+}})} \quad \text{if } Z_E = 2 \tag{7}$$

(" pseudo-Nernstian " metal adsorbate[19]).

As seen in fig. 2, the resulting θ curves each exhibit a sequence of rather drawn out coverage steps that correspond to the voltammetric current peaks of the respective substrate orientations. Attempts to identify a clear-cut correlation between the fully developed steps and hypothetical surface concentrations of simple submonolayer superstructures[20] have been unsuccessful so far except in the (100) system where the total Γ_{Pb} of peak A_1 strongly suggests formation of a $c(2 \times 2)$ Pb single layer.

Characteristically, neither isotherm reveals any θ against E discontinuity, thus indicating perfectly continuous transition from one coverage level to another. Roughly approximating each step individually by a mean field (Frumkin) model, values of the lateral interaction parameter, g, were determined from experimental θ slopes that lie safely within the continuity range of a Frumkin adsorbate[15] ($g_{exp} < 3.5$). Poor step separation also indicates considerable overlap of successive deposition stages.

Such equilibrium behaviour clearly is at variance with the concept of 2D phase-like θ singularities existing in the undervoltage region that undergo first order transformations when E is crossing distinct two-phase coexistence lines. It would, however, support the idea of the Pb deposit occupying continuously a limited number of adsorption sites. Preferential stability of ordered intermediate structures would not be excluded by such a model as long as merging intervals of homogeneity exist which enable the system to establish a steady sequence of θ against E equilibrium states.

Notably, a very similar coverage pattern is observed in Pb undervoltage experiments with single-faced Ag substrates capillary-grown by the Budevski technique.[12,21,22] Minor irregularities notwithstanding, voltammograms taken with this class of electrodes[13] are virtually identical to those obtained with chemically polished macro crystals as far as peak position and peak width is concerned. Thus, basic congruence of the underlying isotherms with respect to both step structure and continuity is demonstrated (fig. 3). Non-discontinuous θ increase particularly may not be attributed to accidental distortion of the evolving monolayer by surface defects such as screw dislocations and subgrain boundaries, as both types of imperfections are absent from Budevski crystals, but appears to be a genuine phenomenon of the regular equilibrium surface.

It is not known to what extent the Pb layer will be influenced by kinks and steps of monoatomic height produced by microroughening when the substrate is exposed to the adsorband electrolyte. Doping Budevski surfaces artificially with Ag growth pyramids which increase the step line density by about 5×10^5 cm/cm^2 was not found to alter the undervoltage properties of Pb appreciably.[13]

POTENTIAL PULSE RESPONSE

At Pb^{2+} concentrations 5×10^{-4} mol dm^{-3} $< c_{Pb^{2+}} < 10^{-2}$ mol dm^{-3}, cathodic potential pulse polarization leads to monotonously decreasing i against t curves regardless of the step width of the voltage signal, provided that $E > E_{Pb/Pb^{2+}}$. The most prominent feature observed is a distinct shoulder which appears when large pulses are applied within the potential ranges of the voltammetric current peaks (fig. 4).

As the current is substantially smaller than that predicted by a semi-infinite diffu-

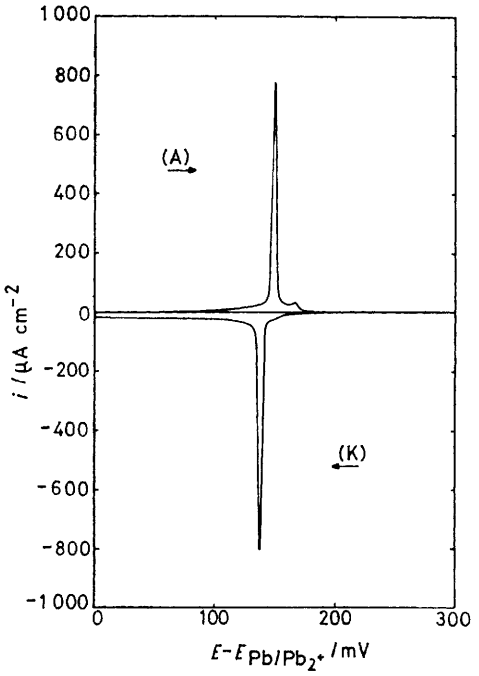

FIG. 3.—Cyclic voltammogram of Pb^{2+} with Ag(111) electrode grown electrolytically by the capillary method. Electrolyte: 0.5 mol dm^{-3} $NaClO_4$ + 0.005 mol dm^{-3} $HClO_4$ + 0.05 mol dm^{-3} $Pb(ClO_4)_2$ $|dE/dt| = 10$ mV s^{-1}.

sion model, the curves cannot be explained by mere transport controlled adsorption.[7] Transients of similar shape and magnitude, however, may easily result from homogeneous first order Pb^{2+} transfer kinetics,

$$d\Gamma_{Pb}/dt = K_{ad(E,\Gamma_{Pb})}(c_{Pb^{2+}} - c_{(E,\Gamma_{Pb})}), \tag{8}$$

assuming K_{ad} varies appropriately with Γ_{Pb}. The $c_{(E,\Gamma_{Pb})}$ parameter denoting the Pb^{2+} equilibrium concentration as a function of E and Γ_{Pb} is defined by the actual θ isotherm. For Frumkin type systems with pseudo-Nernstian θ against E dependence, eqn (8) reads explicitly [*cf.* ref. (7)]

$$d\Gamma_{Pb}/dt = k_{ad}c^{\alpha}_{Pb^{2+}}(1 - \theta)\psi^{\alpha-1} \exp[(1 - \beta)g\theta](1 - a\psi) \tag{9}$$

where $a = k\theta(1 - \theta)^{-1} \exp[-g\theta]$

and $\psi = \exp[2\boldsymbol{F}(E - E_{Pb/Pb^{2+}})/\boldsymbol{RT}]$.

Eqn (9) was used to calculate the pulse response in the main peak region of the Ag(111) system, neglecting the influence of the satellite peaks A_1 and A_3. As seen in fig. 5, remarkable agreement with experiment is thus achieved.

Within the concentration range investigated, rising transients, which might be due to nucleative 2D phase formation, have not been observed. Likewise, asymptotic transient analysis, that would identify non-adsorptive currents in a composite adsorption-nucleation model with 2D phase growth being slow compared with adsorbate relaxation,[23] did not give evidence of coverage processes other than continuous Γ increase according to eqn (8) and (9), respectively.

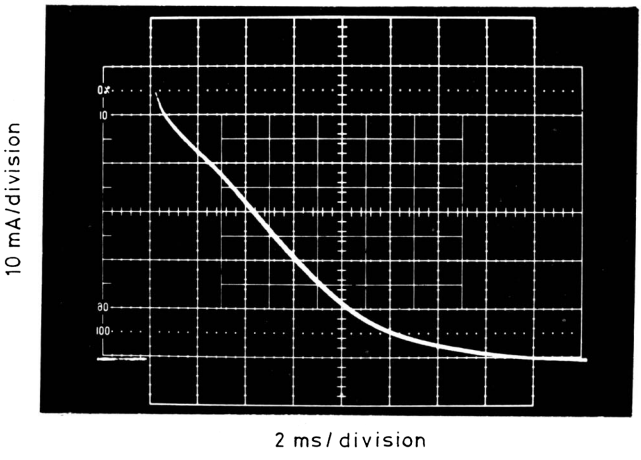

FIG. 4.—Cathodic potential pulse undervoltage transient. Electrolyte: 0.5 mol dm^{-3} $NaClO_4$ + 0.001 mol dm^{-3} H_2SO_4 + 0.01 mol dm^{-3} $Pb(ClO_4)_2$. Electrode: Ag(111), chromate-polished, $E_a = E_{Pb/Pb^{2+}} + 200$ mV; $E = E_{Pb/Pb^{2+}} + 60$ mV.

[*To face page* 20

It is concluded, therefore, that in accordance with isotherm continuity as found voltammetrically, undervoltage deposition kinetics in the Pb^{2+}, ClO_4^-/Ag system is dominated by a homogeneous sorption mechanism, phase formation-like processes being absent or at least kinetically irrelevant.

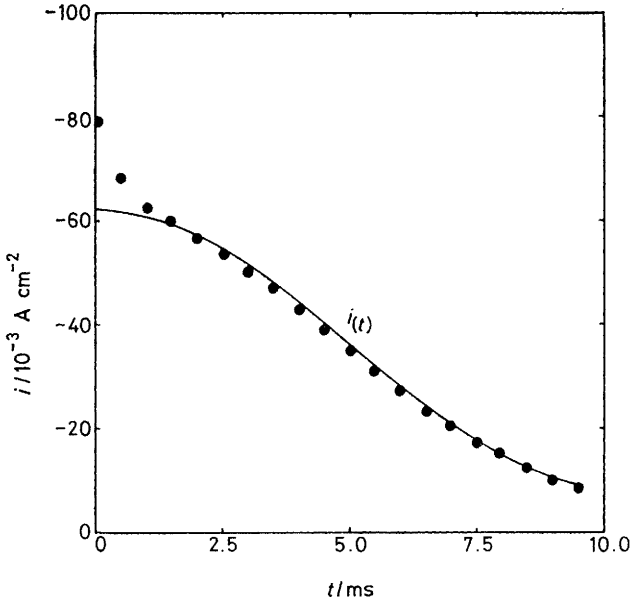

FIG. 5.—Calculated cathodic potential pulse undervoltage transient. ——, Calculated by use of eqn (9): $g = 2.35$; $\alpha = 0.4$; $\beta = 0.6$; $k = 7.47 \times 10^{-5}$; $2\ Fk_{ad}c^{\alpha} = 1.03$ A cm^{-2}; $2F\Gamma_{s,Pb} = 0.38$ mC cm^{-2}. Pulse as in fig. 4. ●, Experimental as in fig. 4.

UNDERVOLTAGE–OVERVOLTAGE TRANSITION

The only nucleative process unambiguously identified in the present system is the onset of Pb bulk phase deposition.

When E is pulsed into the near overvoltage region ($0 > E - E_{Pb/Pb^{2+}} \gtrsim -25$ mV), starting from a low-undervoltage initial potential ($0 < E_a - E_{Pb/Pb^{2+}} < 100$ mV), rising i against t curves are obtained as shown in fig. 6. Their shape appears to be consistent[14] with diffusion controlled 3D nucleation as known from phase growth at polycrystalline Ag.[24,25] The overall current density depends on both the pulse width and the substrate used. In general, i is substantially larger at Ag(100) than at Ag(111).

Phase growth proceeds in the presence of a more or less fully developed undervoltage layer whose Γ_{Pb} increases gradually as the pulse is applied. Therefore, a falling transient is superposed on the nucleative current, establishing (metastable) equilibrium or steady state conditions in the layer within a few tenths of a second. As E_a is close to $E_{Pb/Pb^{2+}}$, the corresponding charge flux usually is small compared with that due to the phase growth process.

There is a remarkable correlation between the overall rate of deposition and the initial state of the undervoltage layer. As seen in fig. 7, the nucleative current decreases sharply when (at constant final E) Γ_{Pb} is increased by shifting E_a towards $E_{Pb,Pb^{2+}}$. Since under such conditions, the growth kinetics of single nuclei is not affected significantly, the rate of nucleation evidently is reduced as Γ_{Pb} approaches

the packing density of the full coverage deposit which is in equilibrium with bulk Pb at $E_{Pb/Pb^{2+}}$.

This almost definitely rules out a closer structural relationship between the bulk phase lattice and ordered 2D domains whose stability and/or frequency increases with Γ_{Pb}, because in that case, enhanced nucleation would result from higher coverage. The most appropriate way to overcome this discrepancy is to assume a major dissimilarity between the 2D layer and the substrate/3D deposit interface. Nucleus formation then would involve a rearrangement requiring a certain intrinsic mobility of the layer. As this structure gradually becomes more rigid by denser packing, nucleation is obstructed, in agreement with experience.

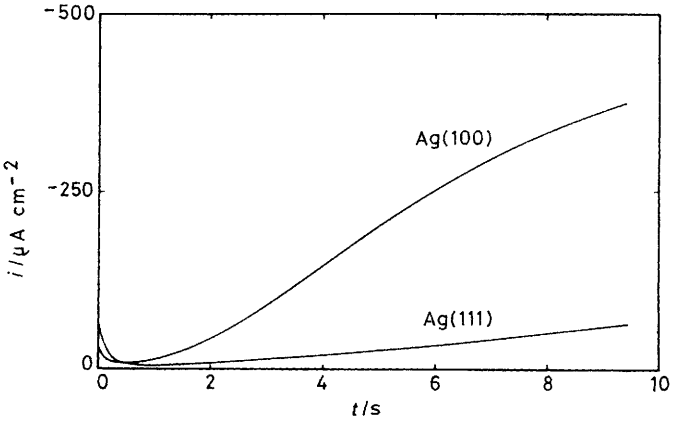

FIG. 6.—Overvoltage potential pulse transients. Electrolyte: 0.5 mol dm^{-3} $NaClO_4$ + 0.005 mol dm^{-3} $HClO_4$ + 0.01 mol dm^{-3} $Pb(ClO_4)_2$. $E_a = E_{Pb/Pb^{2+}} + 75$ mV; $E = E_{Pb/Pb^{2+}} - 16$ mV.

In situ information on the 2D layer, of course, is inaccessible. Substrate/nucleate epitaxy, however, is readily ascertained by Nomarski interference microscopy[26] of deposits obtained with Budevski Ag electrodes. On both (111) and (100) substrates, a limited number of isolated tri- and hexagonal Pb crystallites is seen (fig. 8). From crystal symmetry and edge orientation with respect to the absolute substrate axes, Pb/Ag epitaxy according to

(111)Pb ‖ (111)Ag; [110]Pb ‖ [110]Ag
and (111)Pb ‖ (100)Ag; [110]Pb ‖ [110]Ag

is found. Thus, close-packed [110] lattice rows of both Ag and Pb line up in parallel in the substrate/nucleate interface of either system. As seen from the distances of adjacent [110] rows in the planes involved [Ag(100): 2.88 Å; Ag(111): 2.50 Å; Pb(111): 3.03 Å], the row-by-row misfit in the Pb(111)/Ag(100) system is only 5%, whereas with Ag(111), a 5:6 periodicity is approximated. Both epitaxial structures, consequently, might ensure relatively unstrained contact between Ag and Pb. In view of serious mismatch with natural adsorption sites, however, both row-by-row configurations must be considered inadequate arrangements for continuously evolving 2 D systems which would probably prefer low strain structures such as Ag(100) — $c(2 \times 2)$. Structural identity of 2D layer and substrate/nucleate interface is, therefore, most unlikely.

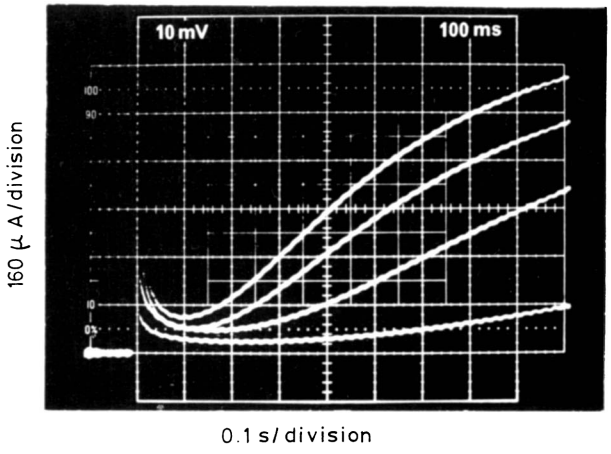

FIG. 7.—Influence of E_a on overvoltage pulse transient. Electrolyte as in fig. 6. $E_a = E_{Pb/Pb^{2+}} + \Delta E$; $E = E_{Pb/Pb^{2+}} - 18$ mV; $\Delta E = 75$ mV (upper curve); 50 mV; 30 mV; 10 mV (lower curve).

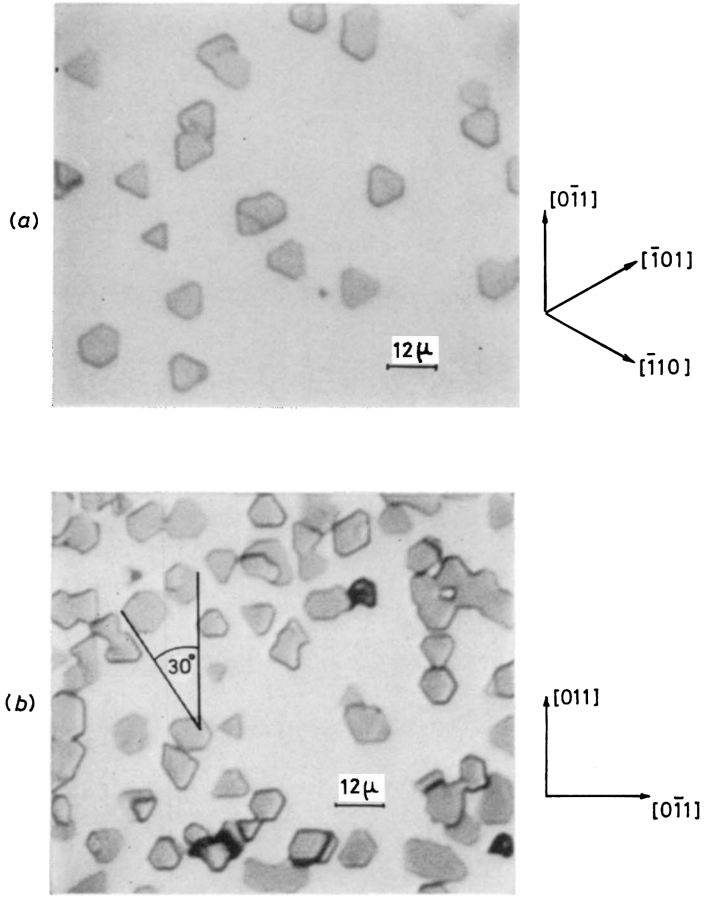

FIG. 8.—Pb deposits at capillary-grown Ag electrodes (Nomarski interference microscopy). Electrolyte as in fig. 6; $E = E_{Pb/Pb^{2+}} - 3$ mV. (*a*) Ag(111); one set of crystallites with parallel edge orientation. (*b*) Ag(100); two sets of crystallites, rotated 30°.

[*To face page* 22

CONCLUSION

The validity in the Pb^{2+}, ClO_4^-/Ag system of the 2D phase concept of metal undervoltage deposition was not confirmed by the experiments reported. Isotherm discontinuities that would positively identify any (first order) 2D phase transition, have not been recognized. Nucleative components of potential pulse i against t undervoltage transients have not been found. Moreover, undervoltage deposition and 3D phase formation appear to be rather disjunct phenomena. Ideally organized 2D layers might even effectively impede 3D nucleation. Homogeneous adsorption models, therefore, are considered more adequate for describing this system.

It should be said, however, that this statement applies strictly to the present investigation. It is not precluded that there might be other systems, or foreign components in the Pb/Ag system such as adsorbing anions which might produce (or mimic) phase transition or nuleation like effects. Further work will help to clarify this issue.

[1] E. Schmidt and H. R. Gygax, *J. Electroanalyt. Chem.*, 1966, **12**, 300.
[2] W. J. Lorenz, H. D. Herrmann, N. Wüthrich and F. Hilbert, *J. Electrochem. Soc.*, 1974, **121**, 1167.
[3] A. Bewick and B. Thomas, *J. Electroanalyt. Chem.*, 1975, **65**, 911.
[4] A. Bewick and B. Thomas, *J. Electroanalyt. Chem.*, 1976, **70**, 239.
[5] J. W. Schultze and D. Dickertmann, *Surface Sci.*, 1976, **54**, 489.
[6] R. Adzic, E. Yeager and D. Cahan, *J. Electrochem. Soc.*, 1974, **121**, 474.
[7] K. Jüttner, G. Staikov, W. J. Lorenz and E. Schmidt, *J. Electroanalyt. Chem.*, 1977, **80**, 67.
[8] H. D. Herrmann, N. Wüthrich, W. J. Lorenz and E. Schmidt, *J. Electroanalyt. Chem.*, 1976, **68**, 273, 289.
[9] A. I. Briggs, H. N. Parton and R. A. Robinson, *J. Amer. Chem. Soc.*, 1955, **77**, 5844.
[10] L. Ramaley and C. G. Enke, *J. Electrochem. Soc.*, 1965, **112**, 947.
[11] E. Schmidt and H. Siegenthaler, *Helv. Chim. Acta.*, 1969, **52**, 2245.
[12] E. Budevski and V. Bostanov, *Electrochim. Acta.*, 1964, **9**, 477.
[13] G. Staikov, K. Jüttner, W. J. Lorenz and E. Budevski, *Electrochim. Acta*, 1977, in press.
[14] G. Staikov, K. Jüttner, W. J. Lorenz and E. Budevski, to be published.
[15] K. Jüttner, H. Bort, W. J. Lorenz and E. Schmidt, to be published.
[16] T. Fukazawa, *cit. Chem. Abstr.*, 1961, **55**, 14279.
[17] A. Bewick and B. Thomas, *J. Electroanalyt. Chem.*, in press.
[18] D. Dickertmann, F. D. Koppitz and J. W. Schultze, *Electrochim. Acta*, 1976, **21**, 1967.
[19] E. Schmidt, *Helv. Chim. Acta*, 1969, **52**, 1763.
[20] F. Hilbert, C. Mayer and W. J. Lorenz, *J. Electroanalyt. Chem.*, 1973, **47**, 167.
[21] E. Budevski, V. Bostanov, T. Vitanov, Z. Stoinov, A. Kotzeva and R. Kaishev, *Electrochim. Acta*, 1966, **11**, 1697.
[22] E. Budevski, V. Bostanov, T. Vitanov, Z. Stoinov, A. Kotzeva and R. Kaishev, *Phys. Stat. Solidi*, 1966, **13**, 577.
[23] G. Staikov, K. Jüttner, W. J. Lorenz and E. Schmidt, *Electrochim. Acta*, 1977, in press.
[24] J. A. Harrison, *J. Electroanalyt. Chem.*, 1972, **36**, 71.
[25] J. A. Harrison, R. P. J. Hill and J. Thompson, *J. Electroanalyt. Chem.*, 1973, **44**, 445.
[26] G. Nomarski and A. R. Weill, *Rev. Metallurg.*, 1955, **52**, 121.